EXPLORING VERY HIGH-RESOLUTION REMOTE SENSING FOR ASSESSING LAND SURFACE TEMPERATURE OF DIFFERENT URBAN LAND COVER PATTERNS

Sh. Asmaryan [1]*, V. Muradyan [1], A. Medvedev [1], R. Avetisyan [1], A. Hovsepyan[1], A. Khlghatyan [1], G. Ayvazyan [1], F. Dell'Acqua[2]

[1] Dept. of GIS and Remote Sensing, Center for Ecological-Noosphere Studies NAS RA,0025, Yerevan, Armenia – (shushanik.asmaryan, vahagn.muradyan, andrey.medvedev, rima.avetisyan, aza.hovsepyan, anahit.khlghatyan, grigor.ayvazyan)@cens.am

[2] Dept. of Electrical, Computer and Biomedical Engineering, University of Pavia, Pavia, Italy – fabio.dellacqua@unipv.it

KEY WORDS: Unmanned aerial vehicle (UAV), very-high resolution remote sensing data, thermal and multispectral remote sensing, land surface temperature, Machine learning models, land cover patterns, Yerevan botanical garden

ABSTRACT:

Very-high-resolution thermal infrared data has a good potential to detect and monitor LST variations in urban areas. In this work, an attempt was made to estimate Land Surface Temperature (LST) from very high resolution (VHR) data using machine learning technics in an area of Botanical garden of Yerevan, Armenia; UAV-derived and in-situ measured high precision LST of various land cover (LC) patterns were then compared for September and October. The main purpose of this study was to explore the capabilities of UAV imagery (multispectral/TIR) in assessing LST of the different LC patterns. For this purpose, a UAV survey was performed, and VHR data were collected using multispectral and TIR thermal camera while in-situ measurements of temperature and surveying of the different LC patterns were performed. A significant correlation was detected between LSTs in situ measured and detected by UAV in 06 September (r=0.758; p-value <0.01) and in 27 October (r=0.686; p-value <0.01). When comparing the LSTs of separate land-cover patterns the best results were received for Bare soils (r=0.591; p-value <0.05) and Concrete (r=0.927; p-value <0.01) when the survey and measurements was done in September. Despite its limitations, it can be stated that UAV thermal survey has a good potential to detect and monitor LST variations in urban areas.

2. INTRODUCTION

The thermal stress in urban areas remains one of the main environmental concerns (Santamouris et al, 2014, Liu et al, 2020). It affects urban ecological processes and urban resident's health and physical comfort (Li et al, 2022, Sodoudi et al, 2018). While people can not manage and control urban climate in large scale, they can improve urban microclimate by planning urban areas and green infrastructure (parks and other green areas). Microclimate is a small-scale climate of near-surface area which is affected by various features of the underlying surface (Shi et al, 2016, Ooka, 2007).

Urban green increases the ability of cities to adapt to climate change by mitigating the effects of the urban heat island (UHI) and therefore heat stress on people (Rahman et al, 2022, Sun et al, 2017). City parks are the main spot for urban residents for recreation and activities like sport, walking with pets, a place for children to play and relax etc. So, comfort of parks - microclimate is one of the main factors of quality of recreation and an important condition when urban residents choose the parks (Bowler et al, 2010, Li et al, 2021).

All these facts point out the importance of urban studies and, in particular, the importance of studying factors determining the comfort of urban environments for residents.

The use of UAVs for urban studies is a considerable advantage, due to spatial, temporal and spectral capabilities of UAV platforms. The capability to derive very high-resolution images and fly on demand integrating multiple sensors make UAVs an important tool for studies in urban areas (Norzailawati Mohd Noor et al 2018, Isibue et al, 2020, Wu et al, 2022).

One of the main factors affecting urban climate including urban microclimate is land surface temperature. Land surface temperature is the heat exchange between earth and the atmosphere. Land surface temperature (LST) highly influence on the formation of this phenomenon and behaves differently based on the various land-cover patterns (Song et al, 2020, Silva et al, 2018, Elachi et al, 2021, Imran et al, 2021).

A high spatiotemporal resolution thermal infrared data provided by an unmanned aerial vehicle (UAV) is a key component when studying the variations of land surface temperature (LST) of different surface types (Feng et al, 2020, Tepanosyan et al, 2021).

In this study an attempt was performed to compare UAV and in situ derived high precision LST of various land cover patterns in an area of Botanical garden of Yerevan (Armenia). For this purpose, high resolution UAV survey was performed and imagery data set was collected using UAV TIR thermal camera and in situ measurements of the different land cover patterns were performed.

3. MATERIALS AND METHODS

3.1 Study site

The study was conducted in the Botanical Garden of Yerevan (Latitude 40.1666, Longitude 44.5166, 1200 m a.s.l.). Yerevan is the capital city of Armenia with an area of approximately 223km^2 and 1.1 million inhabitants, which represents the 36% of the total population and the 56% of urban population. Yerevan lies on a plain on the edge of the Ararat Valley at altitudes of 860–1.400 m. It has a dry continental climate. Summers are long, hot and dry, with average air temperatures between 22.1^{0}C and 25.4 ^{0}C. The absolute maximums of air temperature registered in July are between 40 ^{0}C and 43 ^{0}C (Tepanosyan et al, 2021). The Botanical Garden is one of the main recreational areas and a key element of urban green infrastructure of Yerevan. It covers 80 ha (Kazaryan 1939). UAV and in situ measurements were performed on 6th Sept and 27th Oct. 2022 at noon in a 25-ha area of the garden where

* Corresponding author

https://doi.org/10.5194/isprs-archives-XLVIII-1-W2-2023-1847-2023 | © Author(s) 2023. CC BY 4.0 License.

different land cover patterns can be distinguished easily as follow: (i) asphalt, (ii) concrete areas; (iii) bare soils; (iv) grass covers and lawns; (v) trees.

3.2 UAV survey

UAV surveys were performed on 6th September 2022 and 27th Oct 2022 at noon, when the influence of shadow is minimal according to the highest solar attitude. Flight altitude was 100 m. The imaging site overlap ratio was set to 70% and front overlap ratio was set to 80%.
September and October of 2022 in Yerevan were characterized with high air temperatures. The maximum air temperatures were registered correspondingly 39^{0}C as and 32^{0}C in September and October. So, it was an attempt to capture LST in this season for the further compare with the summer ones. Both days were clear with no cloud.
LST were captured using Zenmuse XT camera mounted on a rigid suspension on the body of the DJI Matrice 200 V2 UAV (Table 1). UAV surveys started at 12:00 and lasts 30-45 mins. Flight altitudes were 100m and the image overlapping ratio was set at 80%. The captured images were processed in DJI Thermal Analysis Tool 3 and LST was calculated using the Pix4D program.
Supervised classification was used for determination of different land cover areas. Classification was performed in ArcGIS Pro using Segmentation and Classification toolset.

Item	Descripton
Name	*Zenmuse XT S*
Weight	387 g
Thermal Imager	Uncooled Vox Microbolometer
Lens Focus	19 mm
Radiometric thermal camera resolution	640*512 pixels
Spectral Band	8-14 µm
Operating Temperature	-20^0 to 50^0
Spatial resolution	17 mkm
Accuracy	+/-0.1^0
Name	*DJI Matrice 200 V2*
Transmission Range	Range 3-8 Km
Maximum Flight Time	38 min
Operating Temperature	-4^0 to 122^0
Wind resistance	12m/s
GNSS	GPS+GLONASS
FOV	Horizontal: 60^0, Vertical: 54^0

Table 1. Specifications of infrared thermometer and UAV

3.3 In situ measurements

In total 91 points were measured, where 56 points were measured on 6 September and 35 points on 27 October. For each land cover type the points are distributed as follow: (i) asphalt (n=17), (ii) concrete areas (n=16); (iii) bare soils (n=29); (iv) grass covers and lawns (n=14); (v) trees (n=15). Fig. 1 shows the view of the measurements.
The in-situ measurements of the temperatures were performed using Dual laser infrared thermometer (accuracy: ± 2.5^{0}C, emissivity: 0.96).
The measurements were performed three times in each point and the average value was calculated to fix the LST of the point (Fig. 2).

Figure 1. The distribution of the measurement points among the landcover patterns

a.

b.

Figure 2. Facilities and fieldworks in Yerevan Botanical garden: a) in situ measurements b) UAV survey

3.4 Comparison between UAV-derived and in-situ-measured LST.

The UAV derived LST were compared with the in-situ measured LSTs to verify the accuracy using Pearson correlation analysis (Linderman, 1980).

In order to study and assess the LST of different components of botanical garden LC patterns, supervised classification of UAV multispectral VIS_NIR imagery was carried out using a Support Vector Machine (SVM) (Mountrakis et al, 2011) classifier. The SVM algorithm is a nonlinear generalization of the Generalized Portrait algorithm (Vapnik and Lerner, 1963). The advantage of SVM is the ability to learn data classification patterns with balances accuracy and reproducibility. The SVM decision function is, more precisely, an optimal “hyperplane” that serves to separate/classify observations belonging to one class from another based-on patterns of information about these observations, called features. This hyperplane can then be used to determine the most likely label for the unseen data. The process of training the SVM decision function comes down to identifying a reproducible hyperplane that maximizes the distance/margin between the support vectors of both class labels. The optimal hyperplane is the one that "maximizes the difference" between classes (Pisner et al, 2020).

The data was typically split into training and testing datasets using a similar cross-validation approach. For training dataset, about 60 polygons (segments) were selected for each class.

Cross-validation rate achieved 0.73 (model accuracy which is based on leave-one-out cross-validation, or LOOCV, method). As a result, 10 LC patterns were separated as in Fig 3.

4. RESULTS AND DISCUSSION

Fig 4 shows the UAV TIR-derived LST images. The picture shows the slight difference between the LSTs registered on 6 September and 27 October. When analyzing the in-situ measured LST, the highest LST was registered for *bare soil* class (53.2^0C on September 6^{th} and 20.84^0C on October 27^{th}). The lowest LST was registered for *grass and lawn* class (29.02^0C in September and 10.64^0C in October). The LST characteristics of each LC pattern derived from UAV images show that the highest value was registered again for the *bare soil* class (47.5^0C in September and 25.03^0C in October). However, the lowest LST was registered for *trees* (29.92^0C and 17.6 ^{0}C September and in October correspondingly).

The correlation analysis was conducted for in-situ measured and UAV-derived LST for the whole studied area as well as for the different LC patterns. Fig. 5 shows a significant correlation between LSTs measured in situ and detected by UAV on September 06^{th} (r=0.758; p-value <0.01) and on October 27^{th} (r=0.686; p-value <0.01). Fig. 6 shows the best results obtained for the various LC patterns, where best results were attained for *bare soil* (r=0.591; p-value <0.05) and *concrete* (r=0.927; p-value <0.01).

It is noteworthy that the significant correlation for the separate land cover patterns was detected for the measurements made in September. Unfortunately, the state is not the same for October. Though the existing significant correlation, expected and revealed between in situ measured and UAV sensed LST of all land cover patterns, no significant correlation is detected for the different land cover types such as trees, grass and lawns and asphalt (See Fig. 7). The reason might be the number of in situ measurements, which was less than those in September.

Table 2 shows the mean LSTs for different land covers for October 27^{th}. As seen from Table, lowest mean LST was observed for Vegetation and Shadow LC patterns (16.8 C and 14.1 C). The LSTs of concrete and asphalt are relatively high. However, unlike other urban ecosystems, the Botanic Garden ecosystem is characterized by not too high temperature of asphalted areas and the difference between the temperatures recorded for asphalt areas and green areas is not large (around 6^0C) between, which may due to the excessive presence of green spaces.

There are similar studies implemented in different geographical conditions. According to Koppen and Geiger climate classification Yerevan classified as BSk climate type, which is characterized as cold semi-arid, with annual precipitation of 357 mm (Kottek et al. 2006). Climate of South Korean Changwon City classified as Cfa, warm and temperate climate with 1307 mm annual precipitation. In this case LST of vegetated land covers is lower than LST of concrete, asphalt and bare soil and the asphalt LST is the highest (Song et al, 2020).

In the study of Naughton and McDonald two different study areas were observed; in Milwaukee, Wisconsin and in El Paso, Texas with climate types Dfa (humid continental, 870 mm of annual precipitation) and BWk (cold desert climate, with 221 mm annual precipitation) correspondingly. The results of this study indicate, that gray surfaces (asphalt, concrete etc) keep more sun heat due to high emissivity and as a result these surfaces typically have the highest LST (Naughton and McDonald, 2019). Thus, Land surface variability is significant and ranged between (3.9–15.8 °C) for common land use types.

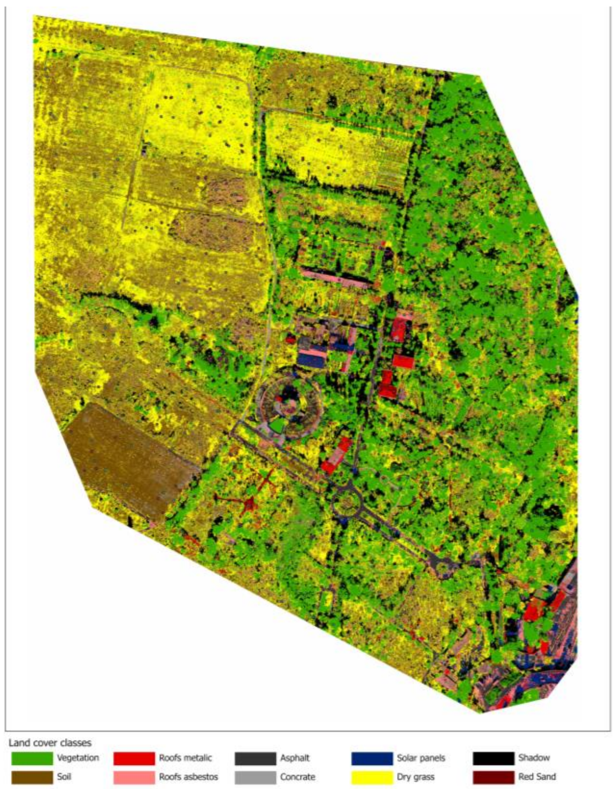

Figure 3. Land cover patterns in the Botanical garden of Yerevan, Armenia generated by SVM pixel-wise classification results using UAV VIS _NIR data for October 27, 2022.

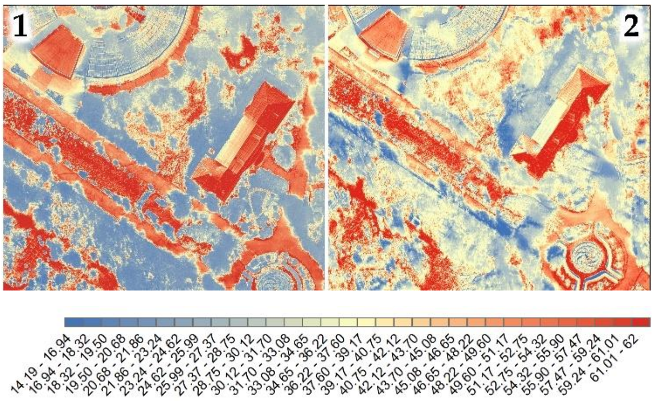

Figure 4. UAV TIR LST derived in (1) September and (2) October

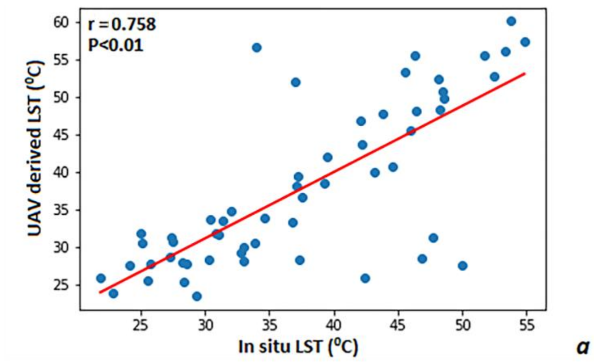

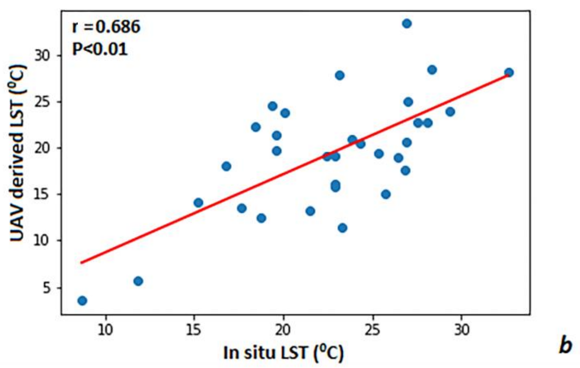

Figure 5. The correlation between in situ measured and remotely sensed LST: a) in 06 September; b) in 27 October

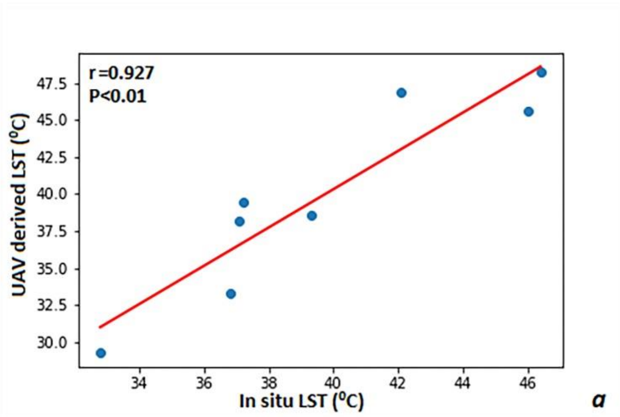

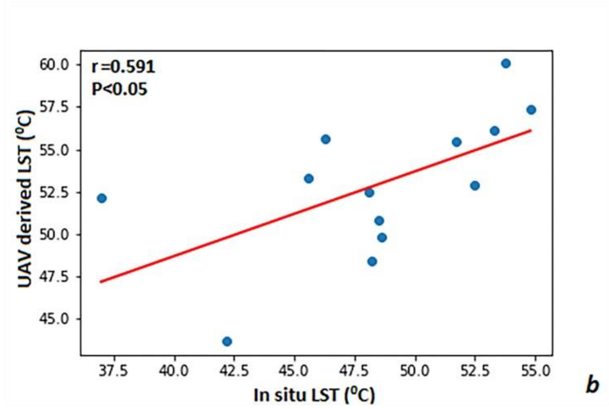

Figure. 6 The correlation between in situ measured (Sept 06) and remotely sensed LST for the separate land-cover patterns: a) concrete and b) bare soils

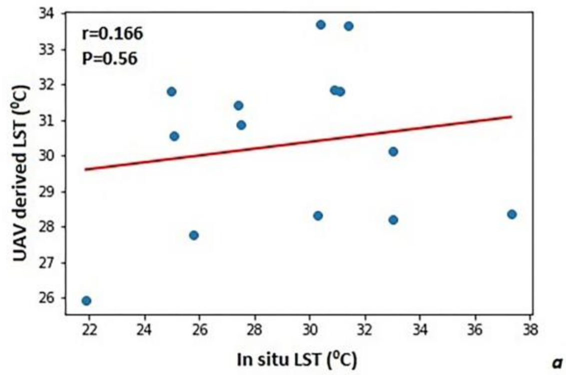

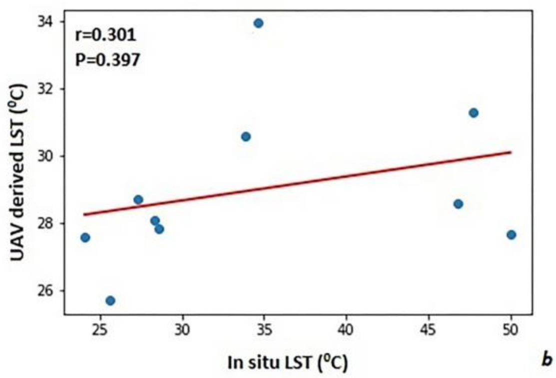

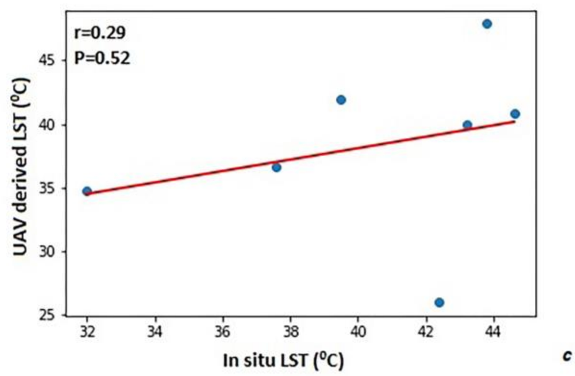

Figure. 6 The correlation between in situ measured (Sept 06) and remotely sensed LST for the separate land-cover patterns: a) trees b) grass and lawns c) asphalt

LST (^{0}C)	LC PATTERNS									
	Red_ Sand	Shadow	Dry_ grass	Solar_ panels	Roofs_ asbestos	Roofs_ metalic	Concrate	Asphalt	Bare Soil	Vegetation
Mean	20.4	14.1	19.2	18.8	19.4	23.3	22.1	21.6	21.3	16.8
Std	9.3	7.0	9.0	11.5	9.7	11.6	10.0	9.1	9.8	7.0
Min	0.0	0.0	0.0	0.0	0.0	0.0	0.0	0.0	0.0	0.0
Median	19.1	13.8	18.4	16.6	18.0	21.6	21.6	21.2	20.7	16.4
Max	45.3	33.6	43.5	52.0	44.9	52.0	49.0	46.5	48.3	25.7

Table 2. Statistical descriptive of LST derived for different LC patterns (October 27)

5. CONCLUSION

Despite the limitations found in this study, such as the scarce number of in-situ measurements in the October campaign, a good correlation has been found between UAV- derived and in-situ measured LST. Also, the reliability of the LST results of the various LC obtained by the SVM model should be noted. This allowed to discover the spatial changes of the relation between the Botanic Garden LC patterns and the LST. It can be stated that VHR UAV-based thermal surveying has a good potential to detect and monitor LST variations in urban areas. Nevertheless, it is also clear that the study should be continued, increasing the quantity of the in-situ measurements and expanding the study period including summer months: June, July and August, when the highest temperatures used to be registered. The alternate to the in-situ measurements by the infrared thermometer is the set of the data loggers, which will provide continuous in situ data series serving an excellent base for the further verification of the accuracy of the UAV LSTs.

6. ACKNOWLEDGMENT

The work was supported by the Science Committee of RA, in the frames of the research projects 20TTCG-1E009 and №.22IRF-04 and in the framework of the research project № 22YSSPD-09 funded by the “Young Scientists’ Support Program” of the National Academy of Sciences of the Republic of Armenia. The Italian contribution was partly funded by MUR – M4C2 1.5 of PNRR with grant agreement no. ECS00000036 (project NODES). The research group also thanks the Yerevan Botanical Garden of the A. Takhtajyan Institute of Botany NAS RA for dedicated support during field works implementation.

REFERENCES

Bowler, D.E.; Buyung-Ali, L.; Knight, T.M.; Pullin, A.S. Urban greening to cool towns and cities: A systematic review of the empirical evidence. Landsc. Urban Plan. 2010, 97, 147–155. https://doi.org/10.1016/j.landurbplan.2010.05.006

Elachi, C.; Van Zyl, J.J. Introduction to the Physics and Techniques of Remote Sensing; John Wiley & Sons: Hoboken, NJ, USA, 2021.

Feng, L., Tian, H., Qiao, Z., Zhao M., Liu, Y., "Detailed Variations in Urban Surface Temperatures Exploration Based on Unmanned Aerial Vehicle Thermography," in IEEE Journal of Selected Topics in Applied Earth Observations and Remote Sensing, vol. 13, pp. 204-216, 2020, https://doi.org/10.1109/JSTARS.2019.2954852.

Imran, H. M., Hossain, A., Islam, A.K.M.S. et al. Impact of Land Cover Changes on Land Surface Temperature and Human Thermal Comfort in Dhaka City of Bangladesh. Earth Syst Environ 5, 667–693 (2021). https://doi.org/10.1007/s41748-021-00243-4

Isibue, E. W., Pingel, T. J. Unmanned aerial vehicle based measurement of urban forests. Urban For. Urban Green., vol. 48, p. 126574, Feb. 2020, doi: 10.1016/j.ufug.2019.126574

Kazaryan, Y. S. Yerevan botanic garden. Academy of Sciences of the Armenian SSR. Botanical Garden. Bulletin, N1. Yerevan, Arm SSR. 1939, pp 7-22

Kottek, M.; Grieser, J.; Beck, C.; Rudolf, B.; Rubel, F. World map of the Köppen-Geiger climate classification updated. Meteorol. Z. 2006, 15, 259–263 http://dx.doi.org/10.1127/0941-2948/2006/0130

Li, J.; Mao, Y.; Ouyang, J.; Zheng, S. A Review of Urban Microclimate Research Based on CiteSpace and VOSviewer Analysis. Int. J. Environ. Res. Public Health 2022, 19, 4741. https://doi.org/10.3390/ijerph19084741

Li, Y., Fan, S., Li, K. et al. Microclimate in an urban park and its influencing factors: a case study of Tiantan Park in Beijing, China. Urban Ecosyst 24, 767–778 (2021). https://doi.org/10.1007/s11252-020-01073-4

Lindeman, R. H., Merenda, P. F., & Gold, R. Z. Introduction to bivariate and multivariate analysis. Glenview, IL: Scott, Foresman and Company 1980

Liu, F., Zhang, X., Murayama, Y., Morimoto, T., Impacts of Land Cover/Use on the Urban Thermal Environment: A Comparative Study of 10 Megacities in China, Remote Sens. 12, 2020, 307. https://doi.org/10.3390/rs12020307

Mountrakis G, Im J., Ogole C. 2011 Support vector machines in remote sensing: A review, ISPRS Journal of photogrammetry and remote sensing. V66, I3, https://doi.org/10.1016/j.isprsjprs.2010.11.001

Naughton, Joseph, and Walter McDonald. 2019. "Evaluating the Variability of Urban Land Surface Temperatures Using Drone Observations" *Remote Sensing* 11, no. 14: 1722. https://doi.org/10.3390/rs11141722

Norzailawati Mohd Noor et al, 2018 Remote sensing UAV/drones and its applications for urban areas: a review IOP Conf. Ser.: Earth Environ. Sci. 169 012003 https://doi.org/10.1088/1755-1315/169/1/012003

Ooka, R. Recent development of assessment tools for urban climate and heat-island investigation especially based on experiences in Japan. Int. J. Climatol. 2007, 27, 1919–1930. https://doi.org/10.1002/joc.1630

Pisner D. A. and D. M. Schnyer, “Chapter 6 - Support vector machine,” in Machine Learning, A. Mechelli and S. Vieira, Eds., Academic Press, 2020, pp. 101–121. https://doi.org/10.1016/B978-0-12-815739-8.00006-7.

Rahman, M.A., Franceschi, E., Pattnaik, N. et al. Spatial and temporal changes of outdoor thermal stress: influence of urban land cover types. Sci Rep 12, 671 (2022). https://doi.org/10.1038/s41598-021-04669-8

Santamouris, M., On the energy impact of urban heat island and global warming on buildings, Energy Build. 82, 2014, pp. 100–113. https://doi.org/10.1016/j.enbuild.2014.07.022

Shi, Y.; Ren, C.; Zheng, Y.; Ng, E. Mapping the urban microclimatic spatial distribution in a sub-tropical high-density urban environment. Archit. Sci. Rev. 2016, 59, 370–384. https://doi.org/ 10.1080/00038628.2015.1105195

Sodoudi, S.; Zhang, H.; Chi, X.; Müller, F.; Li, H. The influence of spatial configuration of green areas on microclimate and thermal comfort. Urban For. Urban Green. 2018, 34, 85–96. https://doi.org/10.1016/j.ufug.2018.06.002

Song, B., Park, K., Verification of Accuracy of Unmanned Aerial Vehicle (UAV) Land Surface Temperature Images Using In-Situ Data. Remote Sens. 2020, 12, 288. https://doi.org/10.3390/rs12020288

Sun, S.; Xu, X.; Lao, Z.; Liu, W.; Li, Z.; García, E.H. Evaluating the impact of urban green space and landscape design parameters on thermal comfort in hot summer by numerical simulation. Build. Environ. 2017, 123, 277–288. https://doi.org/10.1016/J.BUILDENV.2017.07.010

Tepanosyan, G., Muradyan, V., Hovsepyan, A., Pinigin, G., Medvedev, A., Asmaryan, S., 2021. Studying spatial-temporal changes and relationship of land cover and surface Urban Heat Island derived through remote sensing in Yerevan, Armenia. Build. Environ 187, 107390. https://doi.org/10.1016/j.buildenv.2020.107390.

Vapnik, V. and Lerner, A. (1963) A Pattern Recognition Using Generalized Portrait. Automation and Remote Control, 24, 6

Wu Y. et al. Method of calculating land surface temperatures based on the low-altitude UAV thermal infrared remote sensing data and the near-ground meteorological data. Sustain. Cities Soc. 2022. Vol. 78. P. 103615. https://doi.org/10.1016/j.scs.2021.103615